Sulfur Hydrogen Bonding in Isolated Monohydrates: Furfuryl Mercaptan vs. Furfuryl Alcohol

Marcos Juanes,[a] Alberto Lesarri,[a]* Ruth Pinacho,[b] Elena Charro,[c] José E. Rubio,[b] Lourdes Enríquez,[b] Martín Jaraíz[b]

[a]Mr. M. Juanes, Prof. Dr. A. Lesarri, Departamento de Química Física y Química Inorgánica, Facultad de Ciencias, Universidad de Valladolid, 47011 Valladolid (Spain). E-mail: lesarri@qf.uva.es
[b]Dr. R. Pinacho, Dr. J. E. Rubio, Dr. L. Enríquez, Prof. Dr. M. Jaraíz, Departamento de Electrónica, ETSIT, Universidad de Valladolid, 47011, Valladolid (Spain)
[c]Dr. E. Charro, Departamento de Didáctica CCEE, Facultad de Educación, Universidad de Valladolid, 47011, Valladolid (Spain)

Abstract: The hydrogen bonds involving sulfur in the furfuryl mercaptan monohydrate are compared with the interactions originated by the hydroxyl group in furfuryl alcohol. The dimers with water were created in a supersonic jet expansion and characterized using microwave spectroscopy and supporting molecular orbital calculations. In furfuryl alcohol – water a single isomer is observed, in which the water molecule forms an insertion complex with two simultaneous hydrogen bonds to the alcohol (O-H···O_w) and the ring oxygen (O_w-H···O_r). When the alcohol is replaced by a thiol group in furfuryl mercaptan – water two isomers are observed, with the thiol group preferentially behaving as proton donor to water. The first isomer is topologically equivalent to the alcohol analog but the stronger hydrogen bond is now established by water and the ring oxygen, assisted by a thiol S-H···O_w hydrogen bond. In the second isomer the sulfur group accepts a proton from water, forming a O_w-H···S hydrogen bond. Binding energies for the mercaptan – water dimer are predicted around 12 kJ mol^{-1} weaker than in the alcohol hydrate (B3LYP-D3(BJ)). The non-covalent interactions in the furfuryl dimers are dominantly electrostatic according to a SAPT(0) energy decomposition, but with increasing dispersion components in the mercaptan dimers, larger for the isomer with the weaker O_w-H···S interaction.

Introduction

Hydrogen bonds (HBs) to sulfur centers have been conventionally dismissed as weak interactions of dispersive character, with reduced structural influence compared to conventional first-row HBs like O-H···O, O-H···N or N-H···O.[1,2] However, as recently reviewed by Biswal [3] and Wategaonkar,[4] sulfur HBs are multifaceted interactions with several points of interest: 1) Sulfur forms σ and π HBs as donor (S-H···O, S-H···S, S-H···π, etc) and acceptor (O-H···S, N-H···S, etc), 2) Sulfur HBs can be as strong as conventional HBs, 3) Sulfur HBs may display considerable electrostatic character and 4) Sulfur HBs influence structure and function of many proteins and organic crystals. Additionally, interest has grown in recent years to sulfur and other atoms in groups 14-16 acting as electrophilic centers in more general three-center chalcogen, pnictogen or tetrel bonds.[5] In consequence, molecular studies are justified to gain information on the structural, energetic and physical aspects involved in the definition of HBs for low electronegativity atoms like the heavier chalcogens S and Se. Previous information on sulfur HBs comes primary from crystal data[6,7] and theoretical calculations.[8,9,10] Matrix FT-IR[11] and double-resonance UV-UV and UV-IR laser spectroscopy[12] have been applied to selected molecular clusters, providing vibrational evidence of sulfur HBs. However, vibrational information not always results in unequivocal structural information. Alternatively, rotational spectroscopy delivers inertial data directly comparable to theoretical molecular calculations, but its use concerning sulfur HBs is scarce. To date, a small set of intra[13,14] and intermolecular sulfur HB interactions have been analyzed rotationally, including O-H···S,[15] F-H···S,[16] C-H···S,[17] S-H···S,[18] S-H···N[19] and S-H···π,[20,21,22] either in hydrogen sulfide clusters[18-22] or sulfur-containing complexes.[15-17] The generation of intermolecular complexes in supersonic jets may thus

contribute to enlarge the empirical data on sulfur HBs, offering benchmark comparisons with the condensed phase and theoretical calculations.

Here we report on the monohydrated dimers of furfuryl mercaptan (FM···H_2O) and furfuryl alcohol (FA···H_2O), offering competing intra/intermolecular HB possibilities for the furfuryl, thiol and alcohol groups. The furfuryl compounds display a simplified (two-rotor) bi-dimensional potential energy surface, providing alternative O/S/π binding sites and sufficient conformational flexibility to establish different, even simultaneous, HBs with water. Since both FM and FA themselves can be stabilized by O/S-H···O or O/S-H···π intramolecular HBs, the insertion of a water molecule may disrupt the conformational preferences of the bare molecules, offering a possibility to investigate the influence of water addition on the conformational balance and intramolecular hydrogen bonding. The solvation of both furfuryl derivatives will therefore allow comparing the donor/acceptor strength of water against the OH and SH groups. The experiment will be assisted by quantum chemical calculations with different dispersion-corrected density functional theory (DFT) models and the MP2 method, simultaneously assessing the theoretical calculations. Finally, an energy decomposition analysis[2] will be used to examine the underlying basis of the intermolecular interactions originated by the thiol and alcohol groups.

Results

Rotational spectra of FM and FA

As a preliminary step in the analysis of the two hydrates we reinvestigated the rotational spectra and conformational and energetic properties of both FM and FA in a cooled supersonic expansion, extending the previous measurements on thermalized static samples (-15ºC and 5ºC, respectively) conducted in the K_a band (26.5-39.5 GHz). [23,24]

The rotational spectra of the monomers revealed a dominant skew conformation in which the thiol or alcohol groups are nearly perpendicular to the ring plane and the terminal hydrogen atom is oriented towards the ring heteroatom, forming a S-H···O or O-H···O intramolecular hydrogen bond in FM and FA, respectively (+*gauche*/-*gauche* or GG´ in Figure 1 for dihedrals τ_1=S/O-C-C-O and τ_2=H-S/O-C-C, respectively). The second most stable conformation shares the heavy-atom skeleton, but the terminal hydrogen atom points to the ring, consistent with a weak S-H···π or O-H···π hydrogen bond (+*gauche*/+*gauche* or GG). Tables S1-S4 of the Supporting Information (SI) show the predicted atomic coordinates. The energy separation between the two most stable GG´ and GG conformations was previously estimated as 2.3(5) and 1.5(4) kJ mol^{-1}, respectively, for FM[23] and FA.[24] These values are comparable to the theoretical MP2 estimations in Tables S5 and S6 (SI), giving relative Gibbs energies of 1.5 and 1.3 kJ mol^{-1}, respectively. Noticeably, the GG isomer, previously detected in a static sample for the two compounds, was observed in the jet for FM but not for FA. This fact is consistent with a lower interconversion barrier in FA, permitting the conformational relaxation[25] to the global minimum GG´. Interconversion barriers GG´→GG were previously available only for FA[26] (B3LYP) and have now been extended to both molecules in Figure S1 (SI) using MP2. For the most abundant GG´ isomer of FM and FA all ^{13}C isotopologues were detected in natural abundance, together with the ^{34}S and one of the

^{18}O species in FM and FA, respectively. Finally, a new third conformer could be assigned for FM (*trans*/*-gauche* or TG´ in Figure 1). The spectroscopic parameters, effective and substitution structures and transition frequencies for FM and FA are collected in Tables S7-S31 (SI).

Rotational spectra of the monohydrates

We generated the neutral monohydrates of furfuryl mercaptan and furfuryl alcohol coexpanding the ring compounds and water vapor with a pressurized neon carrier gas. The near-adiabatic expansion into an evacuated chamber created the dimers by many-body intermolecular collisions in the vicinity of the nozzle, later freezing the clusters in the transient expansion. The rotational spectrum was analyzed in the region 2-18 GHz, with support from three DFT/ab initio molecular models. The most stable isomers for FM···H_2O and FA···H_2O (and adopted notation) are shown in Figures 2 and 3, with predicted rotational parameters in Tables 1 and 2 (B3LYP-D3(BJ)/def2-TZVP; see Tables S32-S33 for alternative B3LYP-D3/6-311++G(d,p) and MP2/6-311++G(d,p) predictions). For both complexes two types of dimers with water resulted from the conformational search: 1) insertion complexes, in which the water molecule bridges the two polar groups of FM or FA, establishing two simultaneous HBs and closing a seven-membered ring, or, alternatively: 2) addition complexes, in which water is primarily attached to the thiol/alcohol group but not to the endocyclic oxygen, eventually forming secondary weak interactions with the furfuryl ring. Intermolecular interactions between the thiol/alcohol groups and the water molecule may proceed in both cases either through donor (S-H/O-H···O_{water}) or acceptor (O_{water}-H···S/O) HBs. Water may exhibit the well-known donor/acceptor role, while the furfuryl monomers may favor the most stable GG´ or GG conformations or eventually become distorted by hydration. This sum of factors made difficult to establish *a priori* which of the isomers in Figures 2 and 3 could be most

stable. The theoretical calculations predicted close relative energies between all isomers (ΔG < 5-8 kJ mol^{-1} in Tables 1-2 for both FM···H_2O and FA···H_2O), but with different energy orderings depending on the quantum chemical model (compare with Tables S32-S33, SI).

Since the conformational predictions were model dependent and could not totally ascertain the identity of the global minima, the initial spectral surveys of the FM and FA hydrates targeted systematically all the isomers predicted in Tables 1 and 2. In FM···H_2O we observed the spectra from two asymmetric rotors denoted isomers I and II, comprising both μ_a- and μ_b-type *R*-branch (J+1←J, J=0-8, $\mu_a > \mu_b$) rotational transitions (Figure S2, SI). The spectral dataset was fitted to experimental accuracy with a semirigid-rotor Watson's Hamiltonian[27] (S reduction), determining all quartic centrifugal distortion constants (except d_2 for isomer I). In order to check the assignment, we added isotopically labeled $H_2{}^{18}O$ water to the jet. A new spectrum at lower frequencies of the parent species was consistent with the expected shifts in the moments of inertia, confirming unequivocally the spectral identification (Figure S3, ESI). Conversely, the spectrum of FA···H_2O (Figure S4, SI) revealed a single isomer with *R*-branch transitions ($\mu_a > \mu_b > \mu_c$), that was analyzed similarly. The spectral identification was again verified by detection of the $H_2{}^{18}O$ isotopologue (Figure S5, SI). The experimental spectroscopic parameters for FM···H_2O and FA···H_2O are collected in Tables 1-2 and S34-S35 (SI), while the observed transitions are listed in Tables S36-S41 (SI). The observation of the $H_2{}^{18}O$ isotopic species allowed determining the atomic coordinates of the water oxygen atom in the monohydrate for the three detected species. The resulting coordinates obtained from the Kraitchman[28] equations are presented in Tables S42-S43 (SI).

The conformational assignment relied on a comparison of the experimental rotational constants and water oxygen coordinates with the theoretical DFT/ab initio

predictions in Tables 1-2, S32-S33 and S42-S43 (SI). The assignment of the furfuryl alcohol monohydrate FA···H_2O was relatively straightforward, as the rotational constants clearly pointed to the identification of the observed cluster as the insertion complex GG´-W_{da}, predicted as global minimum using B3LYP-D3(BJ). This isomer exhibits a network of two consecutive O-H···O HBs, in which the hydroxyl group acts as proton donor to the water oxygen and water similarly behaves as proton donor to the ring oxygen atom. On the other hand, the conformational assignment of the two observed furfuryl mercaptan hydrates FM···H_2O I/ II was more difficult, as the theoretical predictions were not totally consistent and the rotational constants of the three predicted insertion complexes were relatively close. Finally, inspection of the experimental evidence led to the identification of isomer I as GG´-W_{da} and isomer II as GG-W_{dd}. In both complexes water simultaneously binds to the ring oxygen and to the thiol group, with the thiol group engaging to water either as proton donor (isomer I) or proton acceptor (isomer II). Vibrationally-averaged effective structures were calculated for the three observed dimers by a least-squares fit of the moments of inertia.[29,30] For FA···H_2O we could fit both the position of the water oxygen and the orientation of the water moiety (using an auxiliary dummy atom in the C_2 water axis), satisfactorily reproducing all observed rotational constants with a five parameters fit, as observed in Table S44. For FM···H_2O a reduced set of three parameters adjusting only the water oxygen position was determinable (Tables S45-S46). In all cases the rest of the dimer was frozen at the B3LYP-D3(BJ) geometry. A comparison of the equilibrium, vibrationally-averaged structures and water oxygen substitution coordinates is shown in Figure 4. The atomic coordinates from the effective structure can be compared with the DFT predictions in Tables S47-49.

Discussion

We have examined the non-covalent interactions stabilizing the water adduct of furfuryl mercaptan and observed the binding consequences of replacing a thiol by an alcohol group in the furfuryl monomer. Two isomers of monohydrated furfuryl mercaptan (GG´-W_{da} and GG-W_{dd}) and one isomer of the analog alcohol dimer (GG´-W_{da}) were detected in the isolation conditions of a supersonic jet. Several structural and energetic arguments rationalize these observations. The detection of two different isomers in FM···H_2O is partly due to the different conformational composition of the monomers in the jet. FM and FA display similar preferences for the thiol or alcohol group, with the exocyclic S/O heteroatom *gauche* to the ring (monomer structures in Tables S1-S4, SI) and terminal hydrogen atoms pointing to the ring heteroatom. The thiol/alcohol internal rotation barriers are apparently similar (5.8 vs 4.9 kJ mol^{-1}, respectively, in Figure S1, SI), but the slightly larger value in FM effectively prevents conformational relaxation between the GG and GG´ isomers, since both monomers are detected in the jet. Conversely, the lower interconversion barrier in FA, closer to the empirical threshold of $2kT_{nozzle}$,[25] actually depopulates the higher energy isomer GG by relaxation to the global minimum GG´. The availability in the expansion of two isomers of FM kinetically favors the formation of two different dimers with water, while in FA only the global minimum appears bound to water.

The formation of insertion complexes with a network of two simultaneous HBs is preferred to addition complexes. The strongest HB in the FA monohydrate is formed by the ring alcohol, acting as proton donor to water (O-H···O_w). Simultaneously water binds as proton donor to the ring (O_w-H···O_r), reminiscent of the conformation of the furan monohydrate.[31] The stronger character of the alcohol HB is apparent in the geometry of the complex, with the water oxygen considerably displaced with respect to the furfuryl

plane and shorter hydrogen bond distances to the alcohol group (r(OH···O_w)=1.956(3) Å vs. r(O_wH···O_r)=2.16(1) Å in Figure 4). The O-H···O_w hydrogen bond distance is close to that observed in the gas-phase for water adducts with cyclic ethers and alcohols, where only a main HB is formed (ethylene oxide:[32] 1.92(1) Å; propylene oxide:[33] 1.908(7) Å; oxetane:[34] 1.86(2) Å; tetrahydropyrane: [35] 1.91(2) Å; 1,4-dioxane: [36] 1.90(3) Å; tert-butyl alcohol:[37]1.903 Å). In the FM hydrate the situation is reversed, as evidenced in the bonding distances and the oxygen position, now closer to the furfuryl ring. In isomer I (GG´-W_{da}) the primary HB is now formed by water acting as proton donor to the ring (r(O_wH···O_r)=1.99(2) Å), while the thiol forms a weaker secondary HB (r(SH···O_w)=2.44(3) Å). For comparison, the analysis of the furan monohydrate found an effectively planar dimer with a slightly shorter hydrogen bond (r_{OwOr}=2.8561(18) Å, r(O_wH···O_r)=1.95 Å). [31] The thiol group preferentially behaves as proton donor to water, as observed by comparison of isomers GG´-W_{da} and GG-W_{dd}. The predicted complexation energies favor GG´-W_{da} by 1.0 kJ mol^{-1} (B3LYP-D3(BJ)) to 2.9 kJ mol^{-1} (MP2). When the thiol group behaves as proton acceptor in isomer GG-W_{dd} the water molecule is weakly bound to the sulfur atom (r(O_wH···S)=2.95(3) Å), and the water oxygen similarly sits closer to the furfuryl plane (r(O_wH···O_r)=1.95 Å), as in the furan hydrate. In tetrahydrothiophene-water the only O_wH···S hydrogen bond was found much shorter (r(O_wH···S)=2.37(4) Å).[15] For comparison, in the prototype hydrogen sulfide dimer the hydrogen bond distance is r(SH···S)=2.779(4) Å.[18] However, a systematic structural comparison of gas-phase sulfur HBs is presently not possible considering the limited experimental data. Our results for furfuryl alcohol qualitatively confirm the tendency of aromatic alcohols to behave as proton donors to water,[38] as opposed to aliphatic alcohols,[37, 39] where the alcohol behaves as proton acceptor. Additional comparison with the glycidol monohydrate[40] is worth noting because both an alcohol

and an endocyclic oxygen are available for water binding, making the dimer chemically similar to FA⋯ H_2O. Interestingly, the water insertion in glycidol⋯H_2O produces a considerable (9 degree) rearrangement of the O-C-C-O side chain (a torsional change of 18 degrees was previously reported for the hydrate of 2-aminoethanol[41]). In the FA and FM hydrates the experimental rotational constants were reproduced considering that the monomer is not modified on complexation. The theoretical predictions suggest changes in the S/O-C-C-O dihedral on complexation below 2 degrees.

The computational results emphasize the need to properly account for dispersion contributions for weak non-covalent interactions like the sulfur HBs. The B3LYP functional with the Grimme-Becke-Johnson empirical corrections[42,43] (D3(BJ)) provided a satisfactory approximation to the experimental rotational constants in terms of efficiency and cost. As an example, the relative deviations for FM⋯H_2O I and FA⋯H_2O amount to 0.2-1.2% and 1.1-2.3%, respectively (for comparison the MP2 relative differences represent 0.3-3.2% and 0.5-1.2%, respectively). On the other hand, neither B3LYP-D3(BJ) nor MP2 could correctly identify the global minimum for the mercaptan hydrate and establish a definitive energy ordering. Despite we did not observe any internal dynamics associated to the light water molecule that could introduce interpretational problems, the differences in structural and energetic predictions between the three computational models highlight the real level of uncertainty in the calculations. This indicates that as the HB interactions become weaker the selection of a computational model becomes critical.

We found in Tables 1 and S33-S34 (SI) much larger complexation energies for the B3LYP models than for MP2 (i.e., -27.5, -23.8 and -17.9 kJ mol^{-1}, respectively, for B3LYP-D3(BJ), B3LYP-D3 and MP2 in the GG´-W_{da} isomer of FM⋯H_2O). Previous estimations of binding energies involving sulfur HBs depend considerably on the

molecular groups and calculation level. The complexation energies of dimethylsulfide with methanol or water were estimated at -22.8[9] and -16.1 kJ mol^{-1},[10] respectively, using CCSD(T) and G2-MP2. The binding energies in a series of p-cresol dimers and sulfides are in the range -10.4 to -26.1 kJ mol^{-1}.[3] Noticeably, our predictions indicate a consistent increase in complexation energies of 11.2-12.2 kJ mol^{-1} (B3LYP-D3(BJ)) or 8.2-11.1 (MP2) when passing from the furfuryl mercaptan hydrate I/II to furfuryl alcohol, confirming the weaker character of the interactions involving sulfur in the furfuryl mercaptan adducts. Comparative values have been reviewed,[3] including cases where the sulfur HB strength presents stabilizations energies comparable to the alcohol group.[9]

Finally, information on the nature of the non-covalent interactions in the furfuryl – water dimers was obtained from an energy partition analysis[2] based on symmetry-adapted perturbation theory[44,45] (SAPT), evaluated at the observed geometries. The energy decomposition in Table 3 shows dominant electrostatic contributions for FA···H_2O, FM···H_2O-I and FM-H_2O-II, representing 184%, 196% and 171%, respectively, of the total complexation energy. The dispersion terms are of smaller magnitude, but considerably larger in the sulfur compound than in the alcohol (56%-59% vs 42% of the complexation energy, respectively). Differences can also be observed between the two hydrates of furfuryl mercaptan, with less electrostatic and more dispersion components in the second isomer, which correlates satisfactorily with the structural data. For comparison purposes Table 3 offers additional results for the dimers of water[46] and hydrogen sulfide,[18] together with two clusters dominated by dispersion (pyridine-methane[47]) or mixed-regime (sevoflurane-benzene[48]) forces. In consequence, while the interactions in the three clusters can be categorized as dominantly hydrogen bonding, we appreciate a noticeable decrease in binding energy and larger dispersion character in the interactions involving sulfur.

In conclusion, the synergy between rotational spectroscopy and quantum mechanical calculations has revealed the structural and energetic differences between the thiol and alcohol groups in the furfuryl monohydrates. Rotational data complement the electronic and vibrational experiments in the gas-phase, providing a test-bed for selection and adjustment of molecular orbital methods. Additional theoretical and experimental investigations of other thiol clusters will be necessary to gain a systematic view of the hydrogen bonding and non-covalent interactions involving sulfur.

Experimental and computational methods

The monohydrated FM and FA dimers were created by a near-adiabatic jet expansion of the sample vapors and a carrier gas seeded with water. Neon was used as carrier gas, with backing pressures in the range 1-3 bars (0.8-1.3 mm diameter nozzle). The supersonic jet was probed using both fast-passage[49,50] and cavity[51,52] Fourier-transform microwave (FTMW) spectrometers, covering the frequency regions 2-8 GHz and 8-20 GHz, respectively. In the fast-passage spectrometer (BrightSpec) a microwave chirped pulse (4 μs, 20 W) simultaneously excites the full bandwidth in a single experimental event. In the cavity spectrometer the jet expands within a tuned multi-pass Fabry-Perot resonator and is probed at individual frequencies by bandwidth-limited pulses (1 μs, 0.1 W). The free-induction decay is recorded in the time-domain and Fourier transformed to produce the frequency spectrum. The collinear arrangement of the jet and the resonator axis in the cavity spectrometer results in longer decays and associated smaller linewidths (full widths at half maximum ca. 10 kHz), but restricted to short bandwidths of about 1 MHz. Conversely, the perpendicularly expanding jet in the chirped-pulse experiment produces much shorter decays and enlarges the typical linewidths to about 100 kHz. Frequency oscillators in the two systems are locked to a rubidium standard, providing frequency accuracies of the rotational transitions below 5 kHz.

The experimental work was supported by a combination of molecular mechanics and quantum mechanical methods. The conformational space of the two dimers was first explored with the MMFFs[53] force field, generating a set of plausible initial structures within a 25 kJ mol^{-1} window. All isomers of FM···H_2O and FA···H_2O were later reoptimized using both ab initio (MP2) and DFT (B3LYP). Empirical dispersion terms using the Grimme correction (D3[42]) or Becke-Johnson (D3(BJ)[42]) damping function were added to the B3LYP functional. Vibrational frequency calculations (harmonic

approximation) and basis-set superposition errors were later calculated for each method. The computational models used both Ahlrichs' def2TZVP and Pople's 6-311++G(d,p) triple-ζ basis sets, implemented in Gaussian09.[54] Zero-order symmetry-adapted perturbation theory[2,44] (SAPT(0)) and a truncated double-ζ aug-cc-pVDZ (denoted jun-cc-pVDZ) basis set was used for energy partition in both complexes, as this calculation level is reported to provide acceptable error cancellation.[45] SAPT(0) was implemented in Psi4.[55]

Acknowledgements

Financial support from the MINECO-FEDER (CTQ2015-68148-C2-2-P) is gratefully acknowledged.

Conflict of interest

The authors declare no conflict of interest.

Keywords:

Sulfur Hydrogen bonds, Microsolvation, Rotational Spectroscopy, Supersonic Jets

Sulfur hydrogen bonds: Monohydrates generated in a jet expansion illustrate the hydrogen bonding differences between thiols and alcohols.

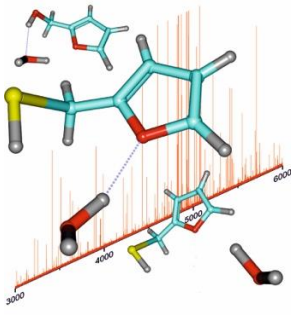

M. Juanes, A. Lesarri,* R. Pinacho, E. Charro, J. E. Rubio, L. Enríquez, M. Jaraíz

Page No. – Page No.
Sulfur Hydrogen Bonding in Isolated Monohydrates: Furfuryl Mercaptan vs. Furfuryl Alcohol

REFERENCES

[1] a) G. C. Pimentel, A. L. McLellan, *The Hydrogen Bond*, W. H. Freeman & Co., London, 1960. b) G. R. Desiraju, T. Steiner, *The Weak Hydrogen Bond in Structural Chemistry and Biology*, Oxford University Press, New York, 1999

[2] S. Scheiner, *Hydrogen Bond, A Theoretical Perspective*, Oxford Univ. Press, Oxford, 1997, and references therein.

[3] H. S. Biswal, Hydrogen Bonding Involving Sulfur: New Insights from Ab Initio Calculations and Gas Phase Laser Spectroscopy, in *Noncovalent Forces* (Ed.: S. Scheiner), Chap. 2, Springer Int. Pub., Switzerland, 2015.

[4] H. S. Biswal, S. Bhattacharyya, A. Bhattacherjee, S. Watergaonkar, *Int. Rev. Phys. Chem.*, 2015, **34**, 99.

[5] a) U. Adhikari, S. Scheiner, *Chem. Phys. Lett.*, 2012, **532**, 31. b) A. C. Legon, *Phys. Chem. Chem. Phys*., 2017, **19**, 14884.

[6] P. Zhou, F. Tian, F. Lv, Z. Shang, *Proteins Struct. Funct. Bioinf*., 2009, **76**, 151.

[7] a) T. Steiner, Angew. Chem. 2002, **41**, 48. b) T. Steiner, Chem. Commun., 1998, 411. c) F. H. Allen, C. M. Bird, R. S. Rowland, P. R. Raithby, *Acta Cryst*., 1997, **B53**, 696.

[8] a) D. L. Crittenden, *J. Phys. Chem. A*, 2009, **113**, 1663. b) A. Vila, R. A. Mosquera, *Int. J. Quantum Chem.*, 2006, **106**, 7440. c) T. P. Tauer, M. E. Derrick, C. D. Sherrill, *J. Phys. Chem. A*, 2005, **109**, 191.

[9] F. Wennmohs, V. Staermmler, M. Schindler, *J. Chem. Phys*., 2003, **119**, 3208.

[10] D. Kaur, D. Aulakh, S. Khanna, H. Singh, *J. Sulfur Chem*., 2014, 35, 290.

[11] a) J. R. Goebel, B. S. Ault, J. E. Del Bene, *J. Phys. Chem. A*, 2001, **105**, 11365. b) M. Wierzejewska, *J. Mol. Struct.* 2000, **520**, 199.

[12] A. Bhattacherjee, Y. Matsuda, A. Fuji, S. Wategaonkar, *ChemPhysChem*, 2013, **14**, 905. b) H. S. Biswal, S. Wategaonkar, *J. Chem. Phys*., 2011, **135**, 134306.

[13] L. H. Xu, Q. Liu, R. D. Suenram, F. J. Lovas, A. R. H. Walker, J. O. Jensen, A. C. Samuels, *J. Mol. Spectrosc*., 2004, **228**, 243.

[14] G. C. Cole, H. Mollendal, J.-C. Guillemin, *J. Phys. Chem. A*, 2006, **110**, 9370.

[15] M. E. Sanz, J. C. López, J. L. Alonso, A. Maris, P. G. Favero, W. Caminati, *J. Phys. Chem. A*, 1999, **103**, 5285.

[16] S. A. Cooke, G. K. Corlett, A. C. Legon, *Chem. Phys. Lett*., 1998, **291**, 269.

[17] E. J. Cocinero, R. Sánchez, S. Blanco, A. Lesarri, J. C. López, J. L. Alonso, *Chem. Phys. Lett.*, 2005, **402**, 4.

[18] a) A. Das, P. Mandal, F. J. Lovas, C. Medcraft, E. Arunan, Comm. FB03, *Int. Symp. Molec. Spectrosc*., Univ. Illinois (Champaign-Urbana, Illinois), 2017. b) F. J. Lovas, Personal communication, 2017.

[19] M. J. Tubergen, J. E. Flad, J. E. del Bene, *J. Chem. Phys*., 1997, **107**, 2227.

[20] E. Arunan, T. Emilsson, H. S. Gutowski, G. T. Fraser, G. de Oliveira, C. E. Dykstra, *J. Chem. Phys.*, 2002, **117**, 9766.

[21] M. Goswami, E. Arunan, *J. Mol. Spectrosc*., 2011, **268**, 147.

[22] M. Goswami, J. L. Neill, M. Muckle, B. H. Pate, E. Arunan, *J. Chem. Phys*., 2013, **139**, 104303.

[23] K.-M. Marstokk, H. Mollendal, *Acta Chem. Scand*., 1994, **48**, 298.

[24] K.-M. Marstokk, H. Mollendal, *Acta Chem. Scand*., 1994, **48**, 25.

[25] a) R. S. Ruoff, T. D. Klots, T. Emilsson, H. S. Gutowsky, *J. Chem. Phys*., 1990, **93**, 3142. b) G. M. Florio, R. A. Christie, K. D. Jordan, T. S. Zwier, *J. Amer. Chem. Soc*., 2002, **124**, 10236.

[26] C. Araujo-Andrade, A. Gómez-Zavaglia, I. D. Reva, R. Fausto, *J. Phys. Chem. A*, 2012, **116**, 2352.

[27] Watson, J. K. G., in *Vibrational Spectra and Structure* (Ed.: J. R. Durig), Vol. 6, pp. 1–89, Elsevier: Amsterdam, 1977.

[28] a) J. Kraitchman, *Amer. J. Phys*., 1953, **21**, 17 b) C. C. Costain, *Trans. Amer. Cryst. Ass.*, 1966, **2**, 157.

[29] H. D. Rudolph, J. Demaison, in *Equilibrium Molecular Structures* (Eds. J. Demaison, J. E. Boggs and A. G. Császár), CRC Press, Boca Raton, FL, 2011, ch. 5, pp. 125–158.

[30] Computer programs MOMSTRUCT, available at: http://www.uni-ulm.de/~hrudolph/

[31] a) F. L. Bettens, R. P. A. Bettens, A. Bauder, Comm. TC05, *Int. Symp. Molec. Spectrosc*., Ohio State Univ. (Columbus, Ohio), 1994. b) F. Bauder, Personal communication, 2017.

[32] W. Caminati, P. Moreschini, I. Rossi, P. G. Favero, *J. Am. Chem. Soc*., 1998, **120**, 11144.

[33] Z. Su, Q. Wen, Y. Xu, *J. Am. Chem. Soc*., 2006, **128**, 6755.

[34] P. Ottaviani, M. Giuliano, B. Velino, W. Caminati, *Chem. Eur. J*., 2004, **10**, 538.

[35] U. Spoerel, W. Stahl, W. Caminati, P. G. Favero, *Chem. Eur. J*., 1998, **4**, 1974.

[36] W. Caminati, A. Dell'Erba, S. Melandri, P. G. Favero, *J. Am. Chem. Soc*., 1998, **120**, 5555.

[37] L. Evangelisti and W. Caminati, *Phys. Chem. Chem. Phys*., 2010, **12**, 14433.

[38] S. Melandri, A. Maris, P. G. Favero, W. Caminati, *Chem. Phys*., 2002, **283**, 185.

[39] a) P. A. Stockman, G. A. Blake, F. J. Lovas and R. D. Suenram, *J. Chem. Phys*., 1997, **107**, 3782. b) I. A. Finneran, P. B. Carroll, M. A. Allodi and G. A. Blake, *Phys. Chem. Chem. Phys*., 2015, **17**, 24210. c) G. J. Mead, E. R. Alonso, I. A. Finneran, P. B. Carroll, G. A. Blake, J. Mol. Spectrosc., 2017, 335, 68.
[40] A. R. Conrad, N. H. Teumelsan, P. E. Wang and M. J. Tubergen, *J. Phys. Chem*. A, 2010, **114**, 336.
[41] M. J. Tubergen, C. R. Torok, R. J, Lavrich, *J. Chem. Phys*., 2003, **119**, 8397.
[42] S. Grimme, J. Antony, S. Ehrlich and H. Krieg, *J. Chem. Phys*., 2010, **132**, 154104.
[43] S. Grimme, S. Ehrlich and L. Goerigk, *J. Comp. Chem*., 2011, **32**, 1456
[44] E. G. Hohenstein, H. M. Jaeger, E. J. Carrell, G. S. Tschumper C. D. Sherrill, *J. Chem. Theory Comput.*, 2011, **7**, 2842.
[45] T. M. Parker, L. A. Burns, R. M. Parrish, A. G. Ryno, C. D. Sherrill, *J. Chem. Phys*. 2014, **140**, 094106.
[46] T. R. Dyke, K. M. Mack, J. S. Muenter, *J. Chem. Phys*., 1977, **66**, 498.
[47] Q. Gou, L. Spada, M. Vallejo-López, A. Lesarri, E. J. Cocinero, W. Caminati, *Phys. Chem. Chem. Phys.*, 2014, **16**, 13041.
[48] N. A. Seifert, D. Zaleski, C. Pérez, J. L. Neill, B. H. Pate, M. Vallejo-López, A. Lesarri, E. J. Cocinero, F. Castaño, I. Kleiner, *Angew. Chem., Int. Ed*., 2014, **53**, 3210.
[49] (a) C. Pérez, S. Lobsiger, N. A. Seifert, D. P. Zaleski, B. Temelso, G. C. Shields, Z. Kisiel, B. H. Pate, *Chem. Phys. Lett*., 2013, **571**, 1; (b) J. L. Neill, S. T. Shipman, L. Alvarez-Valtierra, A. Lesarri, Z. Kisiel, B. H. Pate, *J. Mol. Spectrosc*., 2011, **269**, 21; (c) S. T. Shipman and B. H. Pate, New Techniques in Microwave Spectroscopy, in *Handbook of High Resolution Spectroscopy*, ed. M. Quack and F. Merkt, Wiley, New York, 2011, pp. 801–828.
[50] J.-U. Grabow, Fourier Transform Microwave Spectroscopy Measurement and Instrumentation, in *Handbook of High Resolution Spectroscopy*, ed. M. Quack and F. Merkt, Wiley, New York, 2011, pp. 723–800.
[51] T. J. Balle, W. H. Flygare, *Rev. Sci. Instrum.*, 1981, **52**, 33.
[52] (a) J.-U. Grabow, W. Stahl, *Z. Naturforsch., A: Phys. Sci.*, 1990, **45**, 1043. (b) J.-U. Grabow, W. Stahl, H. Dreizler, *Rev. Sci. Instrum.*, 1996, **67**, 4072.
[53] T. A. Halgren, *J. Comp. Chem*., 1999, **20**, 730.
[54] M. J. Frisch, G. W. Trucks, H. B. Schlegel, G. E. Scuseria, M. A. Robb, J. R. Cheeseman, G. Scalmani, V. Barone, B. Mennucci, G. A. Petersson, H. Nakatsuji, M. Caricato, X. Li, H. P. Hratchian, A. F. Izmaylov, J. Bloino, G. Zheng, J. L. Sonnenberg, M. Hada, M. Ehara, K. Toyota, R. Fukuda, J. Hasegawa, M. Ishida, T. Nakajima, Y. Honda, O. Kitao, H. Nakai, T. Vreven, J. A. Montgomery, Jr., J. E. Peralta, F. Ogliaro, M. Bearpark, J. J. Heyd, E. Brothers, K. N. Kudin, V. N. Staroverov, T. Keith, R. Kobayashi, J. Normand, K. Raghavachari, A. Rendell, J. C. Burant, S. S. Iyengar, J. Tomasi, M. Cossi, N. Rega, J. M. Millam, M. Klene, J. E. Knox, J. B. Cross, V. Bakken, C. Adamo, J. Jaramillo, R. Gomperts, R. E. Stratmann, O. Yazyev, A. J. Austin, R. Cammi, C. Pomelli, J. W. Ochterski, R. L. Martin, K. Morokuma, V. G. Zakrzewski, G. A. Voth, P. Salvador, J. J. Dannenberg, S. Dapprich, A. D. Daniels, O. Farkas, J. B. Foresman, J. V. Ortiz, J. Cioslowski and D. J. Fox, Gaussian 09, Revision D.01, Gaussian, Inc., Wallingford CT, 2013.
[55] R. M. Parrish, L. A. Burns, D. G. A. Smith, A. C. Simmonett, A. E. DePrince III, E. G. Hohenstein, U. Bozkaya, A. Yu. Sokolov, R. Di Remigio, R. M. Richard, J. F. Gonthier, A. M. James, H. R. McAlexander, A. Kumar, M. Saitow, X. Wang, B. P. Pritchard, P. Verma, H. F. Schaefer III, K. Patkowski, R. A. King, E. F. Valeev, F. A. Evangelista, J. M. Turney, T. D. Crawford, C. D. Sherrill, *J. Chem. Theory Comput*., 2017, 13, 3185.

Figure 1. Theoretical Gibbs energies (MP2, kJ mol^{-1}) for the lowest-lying conformations of furfuryl mercaptan (FM) and furfuryl alcohol (FA), as collected in Table S1 (ESI). Molecular conformations are labeled according to the O-C-C-S/O (τ_1) and C-C-S/O-H (τ_2) dihedrals (G= +*gauche*, G´= -*gauche*, T=*trans*).

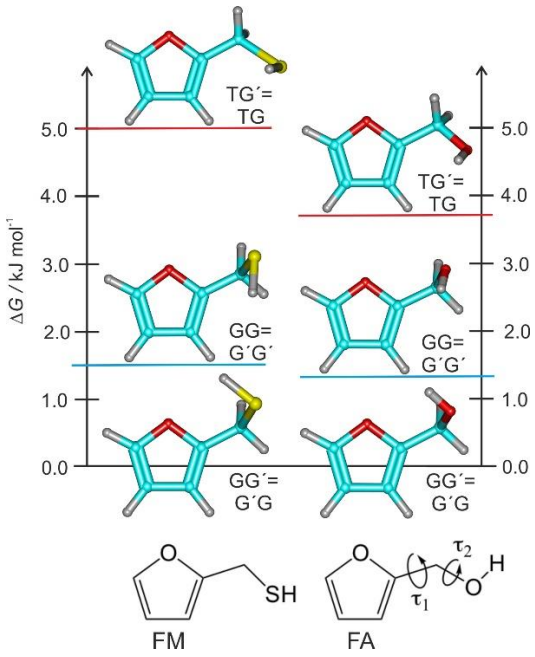

Figure 2. Conformational preferences of the furfuryl mercaptan monohydrate (FM···H_2O), relative Gibbs energies (kJ mol^{-1}) and hydrogen bond distances (Å, B3LYP-D3(BJ)). Isomers are labeled according to the conformation of the monomer (GG´/GG/GT) and the donor/acceptor ($W_{d/a}$) character of water. The red circles indicate the two isomers observed experimentally. Energy values (in red and green) denote the B3LYP-D3(BJ) and MP2 predictions, respectively.

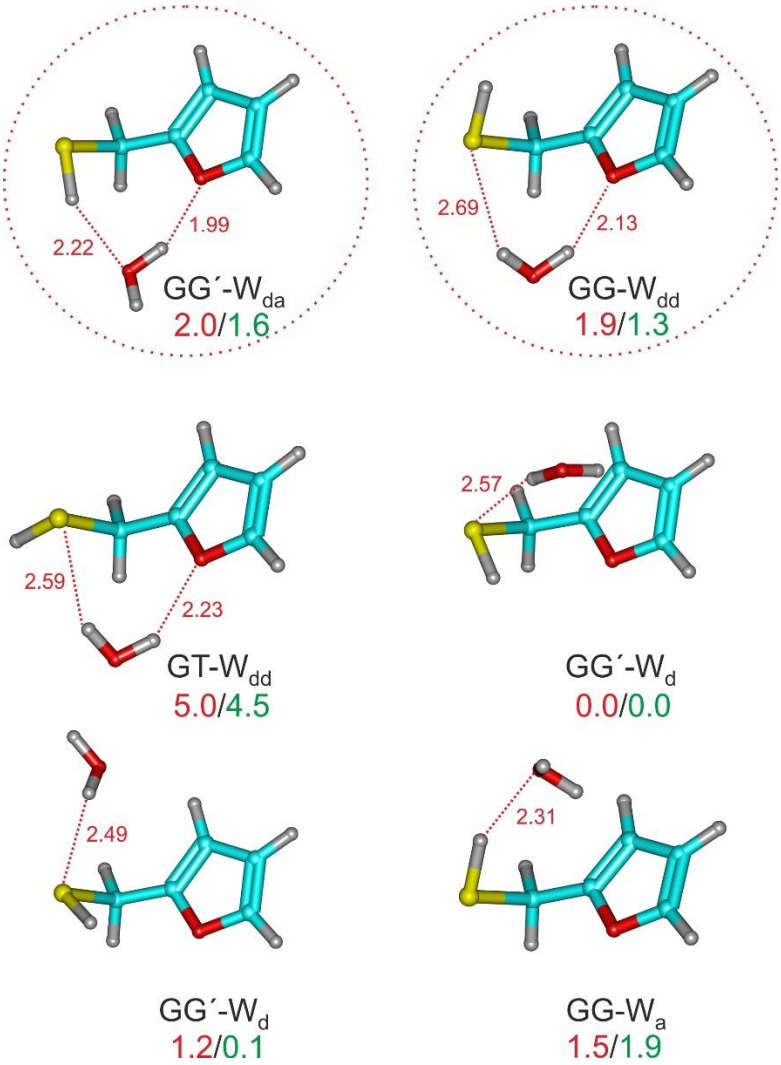

Figure 3. Conformational preferences of the furfuryl alcohol monohydrate (FA···H_2O), relative Gibbs energies (kJ mol^{-1}) and hydrogen bond distances (Å, B3LYP-D3(BJ)). Isomers are labeled according to the conformation of the monomer (GG´/GG/GT) and the donor/acceptor ($W_{d/a}$) character of water. The red circle indicates the only isomer observed experimentally. Energy values (in red and green) denote the B3LYP-D3(BJ) and MP2 predictions, respectively.

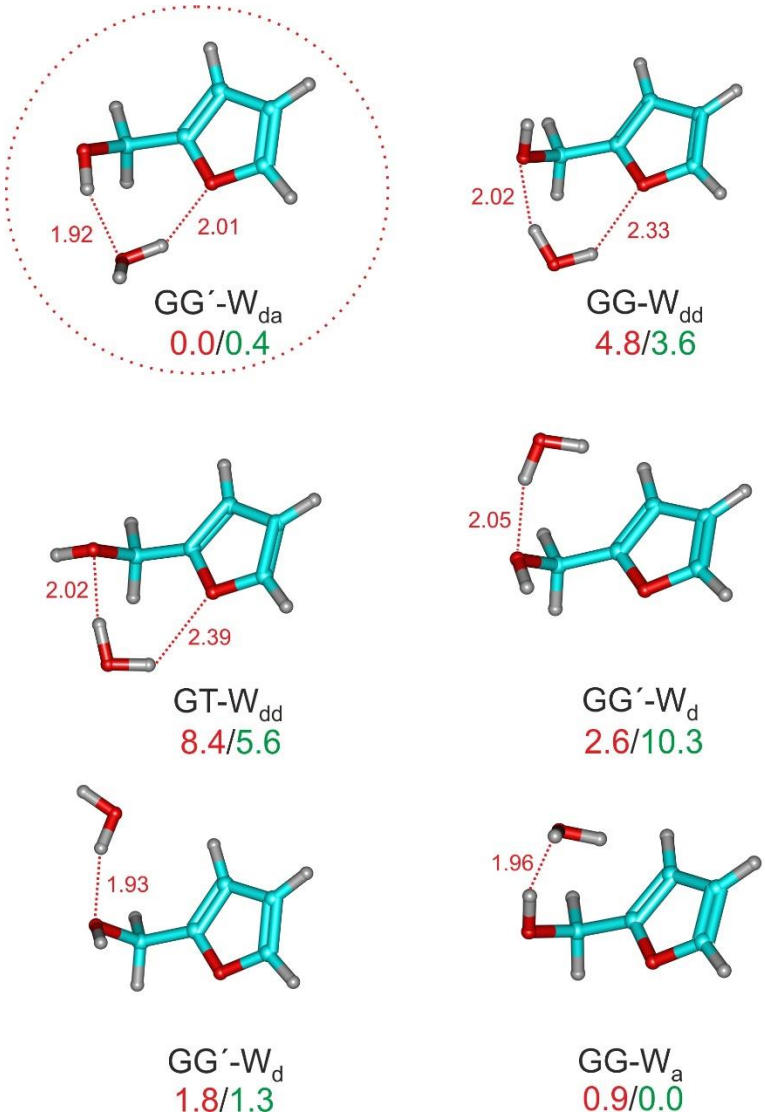

Figure 4. Hydrogen bonding in the monohydrates of furan (top), furfuryl mercaptan and furfuryl alcohol (bottom), comparing the vibrationally-averaged effective structures (solid water molecules), the theoretical predictions (transparent water molecules), and the substitution coordinates of the water oxygen (blue spheres). For the furan hydrate the only structure corresponds to the theoretical calculations (all predictions B3LYP-D3(BJ)/def2-TZVP). The hydrogen bond distances represent both the effective (blue digits) and theoretical equilibrium values (red digits).

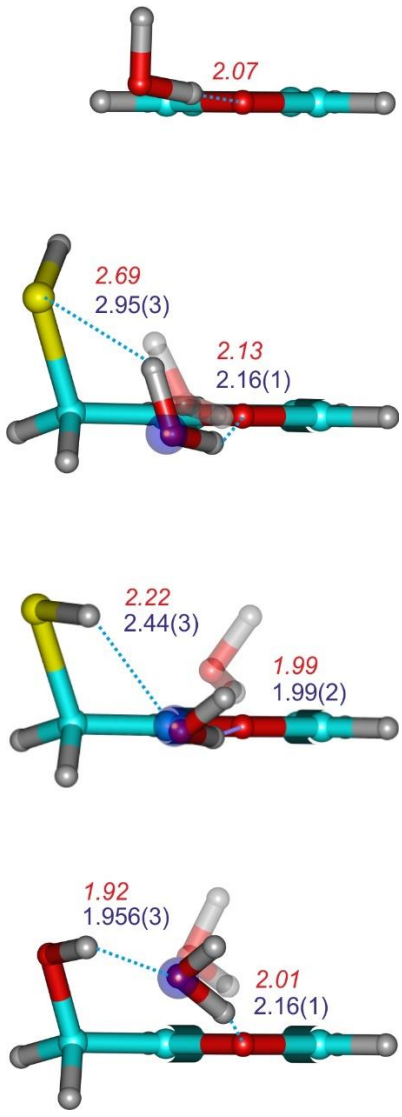

Table 1. Rotational parameters of the dimer furfuryl mercaptan – water.

	Experiment		Theory[f]					
	Isomer I	Isomer II	GG´-W_d	GG´-W_d	GG-W_a	GG-W_{dd}	GG´-W_{da}	GT-W_{dd}
A / MHz[a]	2164.0642(22)[d]	2183.8117(29)	2289.26	2279.40	2214.48	2289.88	2168.91	2307.36
B / MHz	1160.11174(62)	1142.99515(73)	1187.61	1119.12	1171.58	1140.09	1173.86	1139.52
C / MHz	828.46438(29)	830.52727(40)	957.38	826.22	936.03	835.82	823.46	840.96
D_J / kHz	0.1795(44)	0.2285(46)	0.201	0.260	0.390	0.159	0.206	0.179
D_{JK} / kHz	0.409(44)	0.554(49)	1.784	0.940	6.328	0.618	0.929	0.783
D_K / kHz	2.03(18)	5.05(25)	0.883	1.969	-1.058	2.350	3.080	1.625
d_1 / kHz	-0.0236(27)	-0.0599(31)	-0.022	-0.072	0.054	-0.038	-0.070	-0.054
d_2 / kHz	[0.][e]	-0.0184(18)	0.017	-0.020	0.028	-0.012	-0.015	-0.018
$\lvert\mu_a\rvert$ / D	+ + +	+ + +	-1.3	0.0	-2.6	3.1	2.8	2.2
$\lvert\mu_b\rvert$ / D	+	+	-3.3	0.3	-0.8	-2.6	0.4	-2.2
$\lvert\mu_c\rvert$ / D			0.4	-0.4	0.1	0.5	-0.5	0.6
N[b]	29	30						
σ / kHz	9.2	8.3						
ΔE/kJ mol^{-1}[c]			0.0	2.5	3.9	2.9	3.6	5.0
ΔG / kJ mol^{-1}			0.0	1.2	1.5	1.9	2.0	5.0
E_C / kJ mol^{-1}			-23.5	-24.2	-21.5	-22.8	-23.8	-24.7

[a]Rotational constants (A, B, C), Watson's S-reduction centrifugal distortion constants (D_J, D_{JK}, D_K, d_1, d_2) and electric dipole moments (μ_α, α = a, b, c). [b]Number of transitions (N) and rms deviation (σ) of the fit. [c]Relative energies corrected with the zero-point energy (ZPE), Gibbs energy (ΔG, 298K, 1 atm) and complexation energy (including BSSE corrections) relative to the monomers in the geometry of the dimer. [d]Standard errors in units of the last digit. [e]Values in square brackets were fixed to zero. [f]B3LYP-D3(BJ) / def2-TZVP.

Table 2. Rotational parameters of the dimer furfuryl alcohol – water.

	Experiment	Theory					
	FA ⋯ $H_2{}^{16}O$	GG´-W_{da}	GG-W_a	GG´-W_d	GG´-W_d	GG-W_{dd}	GT-W_{dd}
A / MHz[a]	3053.15493(75)	3019.26	2688.69	3218.56	2545.14	3150.80	3117.54
B / MHz	1444.99486(39)	1478.45	1539.60	1300.37	1581.06	1376.40	1400.42
C / MHz	1036.46161(16)	1055.00	1232.59	998.93	1255.77	1016.39	1026.29
D_J / kHz	0.3881(43)	0.42	0.92	0.78	2.05	0.55	0.62
D_{JK} / kHz	-0.289(28)	-0.48	4.47	-2.89	12.29	-1.76	-2.06
D_K / kHz	5.59(14)	6.51	-2.58	10.94	-11.75	8.25	10.74
d_1 / kHz	-0.1252(28)	-0.12	0.01	-0.22	-0.31	-0.19	-0.22
d_2 / kHz	-0.02017(69)	-0.03	-0.02	-0.02	0.06	-0.02	-0.02
$\lvert\mu_a\rvert$ / D	++ +	2.22	-2.65	-0.59	-2.40	4.45	2.52
$\lvert\mu_b\rvert$ / D	++	1.94	-1.88	1.16	2.74	-2.21	2.38
$\lvert\mu_c\rvert$ / D	+	-0.27	-0.09	-0.34	-0.28	-0.63	0.99
N	50						
σ / kHz	5.4						
ΔE / kJ mol^{-1}		0.0	1.4	4.5	5.5	5.7	10.3
ΔG / kJ mol^{-1}		0.0	0.9	1.8	2.6	4.8	8.4
E_C / kJ mol^{-1}		-35.0	-32.1	-29.9	-25.0	-26.2	-26.7

[a]Parameter definition as in Table 1.

Table 3. Binding energy decomposition for the monohydrates of furfuryl alcohol and furfuryl mercaptan (SAPT(0)/jun-cc-pVDZ, kJ mol^{-1}), and comparison with dimers dominated by electrostatic (water dimer), dispersion (pyridine-methane) or mixed (sevoflurane-benzene) intermolecular interactions.

	$\Delta E_{Electrostatic}$	$\Delta E_{Induction}$	$\Delta E_{Dispersion}$	$\Delta E_{Exchange}$	ΔE_{Total}
FM···H_2O – GG´-W_{da}[a]	-41.8	-12.4	-12.9	45.8	-21.3
FM···H_2O – GG-W_{dd}[a]	-35.3	-7.0	-11.8	33.5	-20.6
FA···H_2O – GG´-W_{da}[a]	-61.3	-17.7	-14.6	60.1	-33.4
$(H_2S)_2$ [b]	-12.9	-4.4	-5.2	18.0	-4.5
$(H_2O)_2$[c]	-37.0	-9.0	-5.3	29.4	-21.8
Pyridine-methane[d]	-17.9	-4.1	-42.0	46.1	-17.8
Sevoflurane-benzene[e]	-36.9	-10.5	-37.0	59.4	-25.0

[a]This work. [b]Ref. 18. [c]Ref. 46. [d]Ref. 47. [e]Ref. 48.